Available online at www.CivileJournal.org

Civil Engineering Journal

(E-ISSN: 2476-3055; ISSN: 2676-6957)

Vol. 9, No. 02, February, 2023

Comparison of Methods for Computing Highly Accurate Daily GNSS Positions

Sergey Kuzikov [1*], D. V. Kenigsberg [1], Yuliya Salamatina [1], O. A. Prokhorov [1]

[1] *Research Station of the Russian Academy of Sciences, Bishkek 720049, Kyrgyzstan.*

Received 21 September 2022; Revised 25 December 2022; Accepted 09 January 2023; Published 01 February 2023

Abstract

In Central Asia, the level of geodynamic displacements of the Earth's crust does not significantly exceed the accuracy of their measurement methods. Therefore, we need to choose the most accurate methods of calculating coordinates for cosmogeodetic stations. In this work, based on the data of 8 days of GPS measurements at 10 stations, 7 sets of average daily geocentric XYZ coordinates were calculated using different methods. To determine the positions, we used 3 calculation methods in the GAMIT/GLOBK program, 2 methods in the Bernese GNSS software, and 2 web services. To estimate the differences between 7 coordinate sets, we used parameters based on the Euclidean distance between these coordinate samples. The difference analysis of all pair combinations for 7 coordinate sets was carried out by 3D radius vectors, individual coordinate axes, and individual observation stations. The calculations showed that the positioning accuracy and precision depended not only on the coordinate calculation method but also on the selected reference frame. Methods using the international terrestrial reference frame (ITRF) provide station positions with regular deviations of <2 mm and individual deviations up to 5 cm. Methods using the regional and "point" reference frames have regular discrepancies for individual coordinates up to 2 cm and maximum deviations up to 1 m. Converting XYZ coordinates to UVW with the local reference frame reduces the difference between UVW sets by at least 25%. Due to the spatial orientation relative to the studied stations, the X (U) coordinate is reproduced 2-3 times with smaller deviations than other coordinates. The average deviation level of coordinate sets can be an indicator of the quality of conditions for receiving a GNSS signal at one station. We have identified the station group that has a coordinate deviation level several times lower than other stations.

Keywords: GNSS Coordinate; Position Calculation Method; Reference Frame; Euclidean Distance; GNSS Data Quality.

1. Introduction

The problem of assessing the real accuracy of spatial geodetic positioning is important when measuring small displacements of an observed point on the Earth's surface. Global navigation satellite systems (GNSS) make it possible to obtain object coordinates for different measurement times and error levels. High-precision positioning (with errors up to several mm) is necessary to determine the stability of important engineering objects [1, 2] or to study the movements of the Earth's crust [3, 4]. Based on the coordinate-time series of stations, it is possible to calculate their velocities, kinematic and deformation parameters [5, 6]. Let's define the terms and concepts we use, which are associated with errors in the processing of GNSS data. It is common to characterize GNSS positioning errors in terms of standard deviation or Root Mean Square (RMS). If there are several same type RMS_i for stations, then we can talk about their average and maximum values. In addition to RMS, to describe the properties of coordinate series, it makes sense to give their variation interval, which characterizes the maximum deviation or the difference between the maximum and minimum of coordinate values.

* Corresponding author: ksi-63@yandex.ru

http://dx.doi.org/10.28991/CEJ-2023-09-02-04

Only in a few publications on the analysis of GNSS measurements are two types of error estimates distinguished: *accuracy* and *precision* [7]. Accuracy characterizes the closeness of the result to the true, reference, or expected value. This may be an estimate of the coordinate mean deviation (RMS) for a station in the International Terrestrial Reference Frame (ITRF). Precision determines the proximity of several same-type results to each other. This may be the variation interval for the daily coordinates of one station over several observation days without taking into account their deviations from the true values. Precision can also be expressed in RMS, but this must be specified. Usually, station ITRF coordinates have better accuracy values on a global scale and bad precision, but the accuracy of station coordinates deteriorates (relative to ITRF) in the local reference frame and precision improves [8]. In most cases, for practical technical or geodynamic problems, the precision indicator is more important.

At all GNSS positioning stages, there are factors that can affect the accuracy of the final coordinates. For space geodetic monitoring, three such stages can be distinguished [8]: 1) organization of measuring networks and data collection; 2) data processing; 3) analysis and interpretation of the results.

1.1. Organization of GNSS Network and Measurement Mode

To start conducting high-quality geodetic monitoring, you need to determine the number of observation benchmarks and their locations. For continuous and episodic (repetitive) GNSS measurements, the stability of the antenna relative to the observed object is important. For example, fundamental geodetic benchmarks on the ground or firmly fixed marks on large structures (buildings, dams, etc.) are a better solution than using geodetic tripods to mount the GNSS antenna above the benchmark for positioning accuracy during repeated episodic measurements. It is especially important to have a forced (threaded) antenna fastening to a rigid fundamental base. Insufficient views of the sky (satellites) and the presence of wave-reflecting surfaces can impair positioning accuracy [8, 9]. If the requirements listed above are met when equipping the GNSS benchmark, then such conditions can be considered favorable for geodetic monitoring.

The duration of one position measurement has significant impact on the station coordinates accuracy. The receiver for the measurement epoch records GNSS information in the standard mode every 30 seconds. The more such records (epochs), the more accurately it is possible to determine the average station position for measurement time. For example, the kinematic mode involves short-term measurement intervals of one position (or in motion), which does not give high positioning accuracy. For Real Time Kinematic (RTK), the measurement duration of a single position is reduced to the minimum possible for a given accuracy. The RTK method can increase the accuracy level by increasing the record number per time unit (for example, after 1 second) and receiving corrections from reference stations with accurate coordinates. Sometimes multiple GNSS constellations are used in the RTK method. In the best case, RTK accuracy is estimated through RMS = $\pm$1-2 cm, while the maximum RMS $\geq \pm$5-6 cm [7, 10, 11]. During GNSS measurements of one position for less than a day, the average deviation of coordinates is ±10 mm (up to ±30 mm), measurements lasting more than a day reduce variations in the station coordinates to ±5 mm [12].

The opposite of RTK is the static measurement mode, which involves a long (days, months, years) station measurement. A modern receiver can recognize signals from several GNSS and makes 2880 recordings per day (after 30 seconds). Under favorable station measurement conditions and high-precision standard processing of GPS data (GAMIT/GLOBK), average daily coordinates can be determined in the horizontal plane (N and E) with RMS = ±2 mm and vertically (U) RMS = ±4 mm. In this case, the maximum deviations of the N and E coordinates from the well-known standard can reach 4 mm, and in U up to 9 mm [8].

Modern types of GNSS receivers do not differ significantly in the real accuracy of fixing positioning data [7]. They are capable of recording data from several types of GNSS: GPS (USA), GLONASS (Russia), GALILEO (European Union), BeiDou (China) and others. Data processing methods affect positioning accuracy to a greater extent than the simultaneous use of GNSS different types.

1.2. GNSS Data Processing

Data of field GNSS measurements are converted into files in the RINEX (Receiver Independent Exchange) format, on the basis of which coordinates and velocities are calculated using various programs. The program "GAMIT/GLOBK" and "Bernese GNSS software" (Bernese) are the most well-known and widely used for calculating high-precision coordinates and velocities. The GAMIT/GLOBK software [13] is one of the first scientific programs for calculating high-precision multi-year time series of coordinates and velocities for hundreds of stations in one complex solution. This program initially could work only with GPS data, but its modern versions are capable of complex or separate processing of GPS and GLONASS data. The commercial program Bernese [14] is capable of processing data from GPS, GLONASS and GALILEO navigation constellations at high professional level. Other programs for processing GNSS data have relatively less popularity or accuracy in determining coordinates [15].

If RINEX files contain information from several GNSS constellations, then it is possible to obtain coordinates and velocities based on a complex of these constellations or for each type of GNSS separately. Galaganov et al. [12] analyzed the coordinates calculated by Bernese v5.0 separately from GLONASS and GPS data based on 4 daily observations of station network. In this case, the errors in determining the coordinates (probably precision) according to GPS data are up to 20% less than for GLONASS data. For measurement duration of at least a day, the discrepancy between the coordinates according to GLONASS and GPS data did not exceed 5 mm in ITRF2008.

To analyze the effectiveness of various GNSS for 2017, signal-in-space range errors (SISRE) of 0.2, 0.6, 1, and 2 m are given for Galileo, GPS, BeiDou-2, and GLONASS, respectively [16].

In the experimental work, Shestakov et al. [15], vertical movements of the GNSS antenna were carried out with a step of 6.4 mm every 5 days of measurements. Using the programs Bernese v5.2, GAMIT/GLOBK v10.7 and GIPSY-OASIS v5, the deviations of the measured vertical displacements relative to the known standard were calculated. The results of such a study in RMS are as follows: Bernese (GPS) - 3.3 mm; Bernese (GPS/GLONASS) - 2.9 mm; GAMIT/GLOBK (GPS) - 2.6 mm; GIPSY-OASYS (GPS) - 8.3 mm. The authors note that the calculation of the median for the vertical component gives values closer to the reference results, compared to the RMS calculations.

Based on the data of 7 years of GNSS observations at 34 permanent stations, the velocities were calculated in parallel by the Gipsy-X and GAMIT/GLOBK programs with maximum differences of 0.6 mm/year [17]. In this case, the authors do not compare the coordinates, which may differ significantly from each other, but with a linear approximation they will give close velocities.

Premužić et al. [18] analyzes the data of episodic GNSS observations of the geodynamic network over 4-year period using GAMIT/GLOBK v10.34-6 and Bernese v5.2. At the same time, the coordinate discrepancies between the programs average 2-4 mm, in some cases the deviations reach 2 cm.

In RTK mode positioning efficiency was studied with various combinations of GNSS satellites: GPS, GPS + GLONASS, GPS + GLONASS + GALILEO + BeiDou [10]. The coordinates obtained in the GAMIT/GLOBK program during post-processing were used here as a reference. The coordinates in RTK mode and based only on GPS data have RMS ≈ 2 cm horizontally and RMS ≈ 5 cm vertically. In this study, combinations of multiple GNSS did not have a noticeable advantage in positioning accuracy, and in some cases even worsened it.

For several years of GNSS measurements at more than 200 sites, the coordinates from GAMIT/GLOBK and Bernese have differences at the level of RMS = 2 mm for horizontal and RMS = 4 mm for vertical components under the same initial processing conditions [9]. This study concludes that ambiguities are resolved more successfully when using only GPS data than when combining GPS + GLONASS data.

1.3. Analysis of Positioning Result

Station coordinates are calculated in ITRF using the standard processing strategy in GAMIT/GLOBK or Bernese. In this case, the "conditional observer" is associated with the global group of reference stations (IGS) and is significantly removed from the stations we are studying. It should be taken into account that all average movements and errors from the used IGS reference stations are transferred to the ITRF coordinates of the studied stations. This effect is clearly visible in the transition from ITRF to continental reference systems, for example, to EURA. As a result, the velocity vectors of the Central Asian stations sharply change the general eastern direction to the northern direction and their velocities are reduced by 2-3 times. If the coordinates of the studied stations are converted to local reference system limited only by the studied stations, then we remove the general influence of the external reference frame (for example, ITRF). After that, only movements and errors relative to each other remain in the studied stations coordinates. In the local reference frame, the accuracy of coordinates relative to ITRF is lost, but their precision improves, so it is possible to recognize the reference displacements of stations relative to each other with absolute accuracy up to 1-2 mm [8, 19].

1.4. Conclusions on the Literature Review and Tasks for This Work

From the set of publications presented above, it follows that the errors of GNSS coordinates can be estimated by hitting the target (accuracy) and by the interval of variation (precision). To reduce errors at the level of network organization and equipment of GNSS observation points, the stability of the antenna relative to its initial position and the presence of the maximum open sky are important. The duration of the measurement for one day with 30-second data recording interval in almost all studies provides sufficient accuracy of the GNSS position. As practice shows, the use of data from several GNSS constellations most often does not improve the accuracy of coordinates, and in some cases the accuracy decreases. The duration of one position measurement can also have significant impact on the determination of the benchmark coordinates. The GAMIT/GLOBK and Bernese programs have high level of accuracy when processing GNSS data; the differences for the coordinates and velocities calculated by them usually do not exceed a few mm.

From the foregoing and our professional interest in geodynamic research, the tasks to be solved in this work follow. Modern movements of the earth's crust in most cases are small and imperceptible to humans, and their level of displacements does not always exceed the accuracy of methods for determining the benchmark coordinates. Therefore, any opportunities for improving the quality of positioning at all stages, from field measurements to the analysis of time series of coordinates at the studied stations, are important for us. In this work, we dwelled in detail on the study of comparative accuracy and precision of different methods for calculating GNSS coordinates in the environment of GAMIT/GLOBK v10.71 and Bernese v5.2 programs. In addition, coordinates from 2 web services based on the same input data are subject to research. Here we study the question of the dependence of accuracy and precision of coordinates on their reference frames. For pairwise comparison of sets of coordinates, multidimensional space and its parameters are used, reflecting the average and maximum deviations of the compared data series. We study the issue of improving the accuracy and precision of coordinates in the transition from ITRF to a local reference frame limited only by the stations under study. The structure and types of comparison of methods for calculating positions depending on coordinate systems and with reference to the sections of this work are shown in Table 1.

Table 1. Types of comparison of methods for calculating positions, their coordinate systems and text sections

Comparison type for coordinate calculation methods	Coordinate system (text section)	
On radius vectors	XYZ (4.1.)	UVW (5.1.)
On separate coordinate axes	XYZ (4.2.)	UVW (5.2.)
On individual stations	XYZ (4.3.)	UVW (5.3.)

2. Software and Algorithms for Obtaining GNSS Coordinate

Based on GNSS observations, precision daily coordinates of stations can be computed in Bernese GNSS Software, GAMIT/GLOBK and online-tools. The Bernese GNSS software allows you to estimate the coordinates of stations with high accuracy (determining the spatial position) and precision (reproducing the result). This is possible due to auxiliary input data (satellite clocks and orbits corrections, ionospheric and tropospheric signal delays, tidal loading effects, reference to ITRF, etc.). From the Bernese software we used two methods for obtaining daily positions of sites.

A "Precise Point Positioning" (B3P) is the first method that uses a "zero difference" algorithm in signals between one satellite and one station [14]. The B3P method is configured by default for computing daily average and kinematic (intraday) coordinates. A second method in Bernese software is called "Rinex2Sinex" (BRS). Its main purpose is to provide daily mean coordinates, but it can be configured to compute positions for each measurement epoch. The algorithm "two satellites – two stations" or the “double difference” is used here [14].

Another software package GAMIT/GLOBK is also designed to provide high-precision station coordinates. As well as Bernese software, it uses auxiliary input data for more precise computation of coordinates and velocity vectors. The GAMIT/GLOBK has many different options to set up, but we have chosen three methods for calculating daily positions.

A first method uses default options as well as the necessary files to handle earthquakes or other discontinuities in the observation series [13]. This method uses additional data of nearby IGS stations to stabilize the coordinate time series of the stations we observe. We call this method GAMIT/GLOBK Standard Processing (GSP). A second method does not use input information about ITRF and IGS stations. Therefore, this method from GAMIT/GLOBK is codenamed No Global information (GNG). In this case, a regional reference frame (RRF) consisting of 10 processed stations is used. The other input auxiliary data (atmospheric delays, clock corrections, ground motion parameters, etc.) used here as well. We use the GNG method to evaluate the effect of ITRF and IGS stations on positioning accuracy.

The GAMIT/GLOBK has a special program called TRACK (GTR). Its purpose is to provide kinematic coordinates for each individual epoch. Using the arithmetic mean formula, you can independently calculate the position of the station per day. To process RINEX observation files, this program uses only daily orbit corrections for satellites (*.SP3) as input auxiliary data. However, compared to most GNSS data processing methods TRACK has slightly lower coordinates calculation accuracy. This is due to the fact that the accuracy of the calculated coordinates depends on the relative position of the processed stations. The greater the distance between the stations, the less accurate the coordinates provided. This positioning method corresponds to the level of positioning accuracy in kinematic mode for geodetic and construction work.

We also used two online tools for processing GNSS observation data, in addition to the GAMIT/GLOBK and Bernese programs. These online-tools use all the necessary corrections to calculate the exact coordinates of the site anywhere in the world. One such service is "Canadian Spatial Reference System Precise Point Positioning, CSRS-PPP" (W3P), which processes RINEX files and returns an average daily station coordinates via email [20]. Another online service "The Automatic Precise Point Service of the Global Differential GPS System, APPS" (WPP) is similar to the previous method [21]. However, it is faster at uploading source files to the server and returns the result without email.

The above methods for calculating coordinates use three different reference frames (RF). The B3P, BRS, GSP, W3P and WPP methods use the global ITRF 2014 (ITRF). The GNG method uses a regional RF (RRF) based on 12-13 IGS points closest to Bishkek (13-56° N and 48-104° E), spaced in the northern direction at ~5200 km and eastward at 4800 km. The GTR method uses a "Point" Reference Frame (PRF), which relies only on POL2 station. The daily a priori coordinates for the POL2 station are calculated in GLOBK. For the TRACK program, reducing the distance between the processed points has a positive effect on the precision of the calculation. TRACK software provides satisfactory positioning results if the distance between stations is <100 km. In our case 10 stations are distant from each other up to 1100 km.

3. Source Data for the Comparative Analysis

The methods under study compute different coordinates using the same GNSS input data. And we can estimate the discrepancy between the coordinates calculated by different methods. We need to choose the amount of input GNSS data in order to correctly estimate the coordinate divergences from the calculation methods under study. A large amount of input data has a positive effect on how correctly the methods were compared. But a large amount of input data will be processed for a long time, and the results will be difficult to analyze. Therefore, only 10 stations of permanent measurements of the Central Asian GPS network [8, 22] were selected: IATA, CHUM, KAZA, KRTV, POL2, POL3, POL7, POLY, SUMK, TALA (Figure 1).

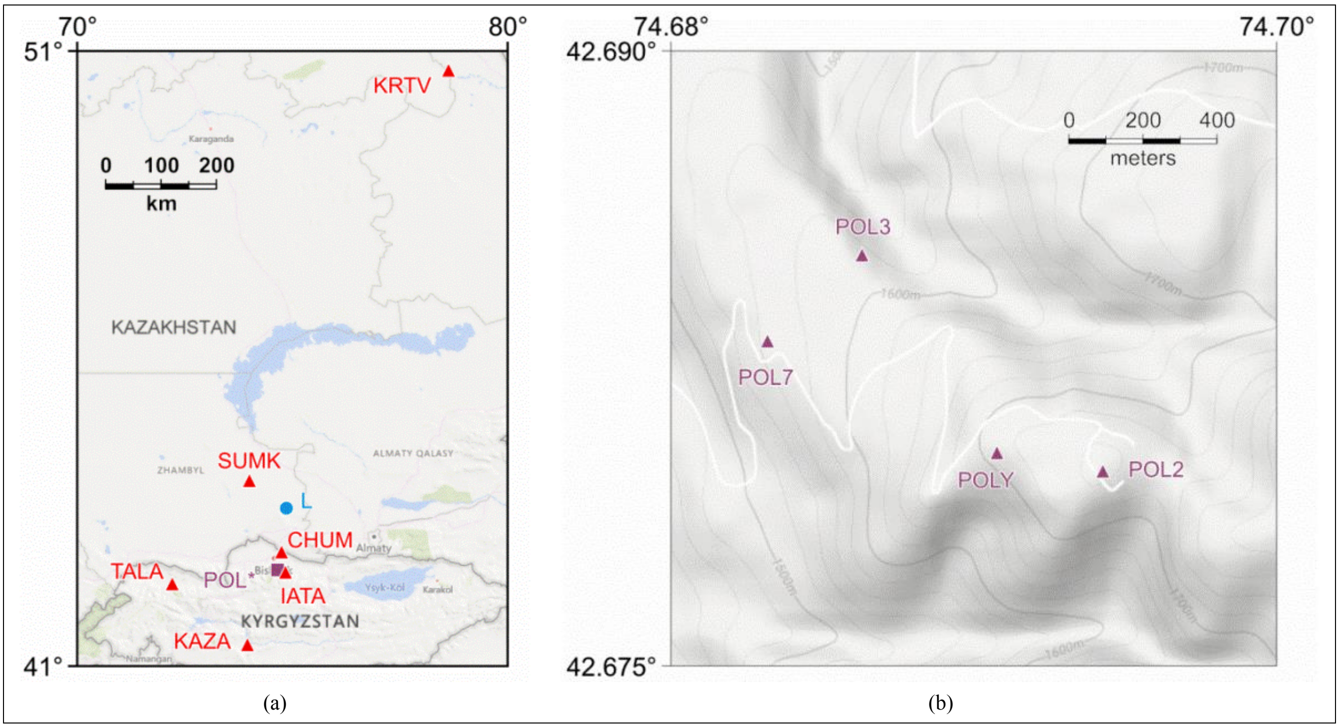

Figure 1. The position of the studied 10 stations on the territory of the Central Asian network: a) 6 GNSS stations with a maximum distance up to 1100 km, POL* – POLIGON geodetic area; b) 4 GNSS stations at the POLIGON area, located 20 km south of Bishkek (Kyrgyzstan).

We chose 2 days at the end of each of the 4 seasons of the year (8 days) for study: November 23-24, 2019; February 11-12, May 21-22, August 22-23, 2020. Thus, 1680 unique coordinates are available for comparison (3 XYZ × 8 days × 10 stations × 7 methods).

The objective of this work is to compare an average daily (daily) coordinates calculated by the above 7 methods. Such an analysis can be done in the geocentric Cartesian coordinates XYZ and in the local coordinate system UVW with origin L (Figure 2).

We can estimate the divergence of global XYZ coordinates in different reference frames (ITRF14, RRF, and PRF). The UVW coordinates are defined in the Local Reference Frame (LRF) for each method. A divergence for the UVW coordinates from different calculation methods is determined relative to L fixed point. The XYZ coordinates have the best accuracy relative to ITRF and the worst precision of station positions relative to each other. The UVW coordinates have lower accuracy and higher precision.

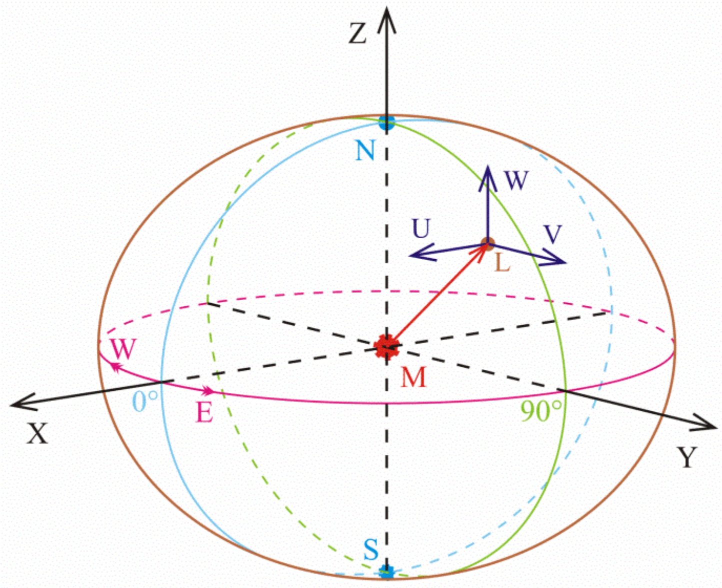

Figure 2. Position of XYZ (geocentric Cartesian) and UVW (local) coordinate systems relative to Earth's ellipsoid; X||U, Y||V, Z||W. The M point is the center of mass of the Earth and the origin of XYZ. The points N and S are the north and south poles of the Earth, lying on the Z axis. The X-axis is the intersection of the planes of the equator and the prime meridian. The Y-axis is the intersection of the equatorial and 90°-meridian planes. The W and E arrows are the west and east directions along the equator. The L point is the mean position of 10 GNSS stations for each day, aligned with the UVW origin.

4. Divergence in Global Geocentric XYZ Coordinates

A general comparison can give one criterion of similarity-differences for 2 methods over the entire volume of analyzed data. A detailed analysis can give an estimate of the divergence along separate coordinate axes or individual stations.

4.1. General Differences between Methods Based on Radius Vectors Deviations

We chose the Euclidean distance as a measure of similarity-difference in order to get the most general result for comparison of methods. The Euclidean distance uses a multidimensional space. Kuzikov et al. [5], 240 coordinates were compared simultaneously for 2 calculation methods. In this work, $\vec{V}(x,y,z)$ radius-vector (3D position similar to vector $\overrightarrow{ML}$, Figure 2) is the unit of multidimensional space and fixes the daily position of one station. A sequence of such vectors forms n-dimensional space (n = 10 stations × 8 days = 80) for each method according to Table 2.

Table 2. Formation of vector pairs for compared methods for 8 days (D1-D8) and 10 stations (S1-S10)

Method code, vector	Order and accordance of vectors							
B3P, $\overrightarrow{\boldsymbol{V1}}(x,y,z)$	$\overrightarrow{\boldsymbol{V1}}_{D1}^{S1}$	$\overrightarrow{\boldsymbol{V1}}_{D1}^{S2}$	…	$\overrightarrow{\boldsymbol{V1}}_{D2}^{S1}$	$\overrightarrow{\boldsymbol{V1}}_{D2}^{S2}$	…	$\overrightarrow{\boldsymbol{V1}}_{D8}^{S10}$	*ED*, *ed*, *edm*
GSP, $\overrightarrow{\boldsymbol{V3}}(x,y,z)$	$\overrightarrow{\boldsymbol{V3}}_{D1}^{S1}$	$\overrightarrow{\boldsymbol{V3}}_{D1}^{S2}$	…	$\overrightarrow{\boldsymbol{V3}}_{D2}^{S1}$	$\overrightarrow{\boldsymbol{V3}}_{D2}^{S2}$	…	$\overrightarrow{\boldsymbol{V3}}_{D8}^{S10}$	

The Euclidean distance from Table 2 will be calculated in the XYZ:

$$ED = \sqrt{\sum_{i=1}^{n}\left(\overrightarrow{V1}_i - \overrightarrow{V3}_i\right)^2} = \sqrt{\sum_{i=1}^{n}\left((x1_i - x3_i)^2 + (y1_i - y3_i)^2 + (z1_i - z3_i)^2\right)} \tag{1}$$

where $\overrightarrow{V1}_i$ and $\overrightarrow{V3}_i$ – are ordered vectors (Table 2) for B3P and GSP methods, respectively.

The *ED* parameter is the sum of absolute differences for n=80 pairs of vectors calculated by two methods. Additional and more detailed information can be obtained on two other criteria. The *regular divergence* (*ed*) is the Euclidean distance (*ED*) divided by the dimension of this space (*n*). The *maximal divergence* (*edm*) is the maximum distance between positions from two different methods:

$$ed = \frac{\sqrt{\sum_{i=1}^{n}\left(\overrightarrow{V1}_i - \overrightarrow{V3}_i\right)^2}}{n}, \quad edm = \sqrt{Max\left(\left(\overrightarrow{V1}_i - \overrightarrow{V3}_i\right)^2\right)} \tag{2}$$

The *ed* and *edm* values for all possible combinations of pairs of methods under study are presented in Table 3.

Table 3. Values of *ed* and *edm* for 21 pair combinations of 7 methods of calculating vectors

ed, mm / *edm*, mm	B3P	BRS	GSP	GNG	GTR	W3P	WPP
B3P		0.69	1.90	44.14	54.38	0.53	1.12
BRS	17.67		1.90	43.97	54.26	0.69	1.26
GSP	40.08	44.70		44.70	54.23	1.82	1.74
GNG	519.27	513.31	513.24		53.46	44.13	44.43
GTR	1406.45	1409.65	1390.58	1444.66		54.34	54.42
W3P	12.18	15.07	39.33	518.33	1405.30		1.03
WPP	27.91	34.70	30.48	522.92	1400.69	28.42	

Method group B3P+W3P+BRS+WPP+GSP has *ed*<2 mm and *edm*<45 mm at 3D positions by visual analysis in Table 3. The GTR and GNG methods have the largest divergence in 3D positions, which reaches 1445 mm.

We used the "Unweighted Pair Group Method with arithmetic Averages" (UPGMA) to group the units (methods) from Table 3 [23, 24]. First, we use the UPGMA algorithm to find the minimum value of *ed*=0.53 and combine the B3P and W3P methods into one cluster. After that, instead of 2 separate rows and columns B3P and W3P, one row and one column B3P+W3P will appear in Table 3. The table cells of the new B3P+W3P cluster will contain the arithmetic averages for the values of the B3P and W3P methods. Then the cycle is repeated with the search for a new minimum value *ed*, and on its basis the cluster of the next level will be formed. This procedure of pairwise union of units can continue until a single cluster is formed, which includes all initially isolated objects according to the parameters *ed* and *edm* (Figure 3).

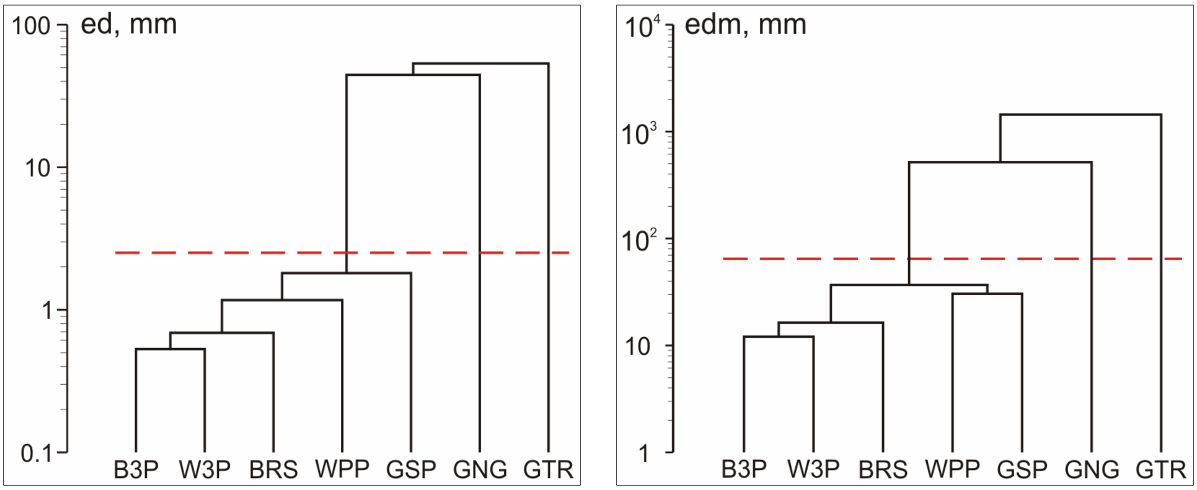

(a) (b)

Figure 3. Dendrograms show the sequence and levels of combining methods into clusters based on criteria: a) regular (average) divergences of vectors between methods (*ed*); b) maximal divergences of radius vectors from different calculation methods (*edm*). The vertical axes are on a decimal logarithmic scale. Dashed lines are expert levels of clustering termination.

The red dashed lines are drawn between the two clustering steps with significant increments between union levels. Based on expert opinion, at this level of similarity measure, you can stop the process of clustering. As a result of the clustering procedure, Table 3 is transformed into Table 4.

Table 4. The clusters of regular and maximal divergences based on 7 methods

ed, mm / *edm*, mm	((B3P+W3P=12.18)+BRS=16.37)+(GSP+WPP=30.48)=36.82	GNG	GTR
(((B3P+W3P=0.53)+BRS=0.69)+WPP=1.17)+GSP=1.81		44.47	54.30
GNG	517.06		53.46
GTR	1401.70	1027.53	

The order of *ed* and *edm* clustering is slightly different, but it doesn't matter. The complex cluster includes 5 positioning methods: B3P, W3P, BRS, WPP, GSP. It is formed at the regular divergence of 1.8 mm and the maximal divergence of 36.8 mm. Small regular divergences in positions for the 5 methods of complex cluster indicates a high level of ITRF coordinates accuracy. The other 2 methods have significant divergences up to 5.5 cm in *ed* and up to 1.5 m in *edm* at positions with other clustering units. The GNG method is limited to RRF and the GTR method is limited to PRF, these reference frames have low accuracy in XYZ.

4.2. Coordinate Stability along Individual X-Y-Z Axes

In addition to deviations in 3D positions, it is also possible to determine the differences from method to method along individual coordinate axes. For each separate coordinate we will form an 80-dimensional range of values (10 stations × 8 days). The scheme for constructing such samples can be shown on the example of the *X* coordinate (Table 5).

Table 5. Forming coordinate pairs to compare *X* values calculated by different methods

Method code, coordinate	*X* value						
B3P, *X1*	$x1_{D1}^{S1}$	$x1_{D1}^{S2}$	…	$x1_{D2}^{S1}$	…	$x1_{D8}^{S10}$	*ED* *ed* *edm*
GSP, *X3*	$x3_{D1}^{S1}$	$x3_{D1}^{S2}$	…	$x3_{D2}^{S1}$	…	$x3_{D8}^{S10}$	

The same principle is used to build rows for Y and Z. The parameters *ED*, *ed* and *edm* for Table 5 will be calculated as follows:

$$ED = \sqrt{\sum_{i=1}^{n}(x1_i - x3_i)^2}, ed = \frac{ED}{n}, edm = \sqrt{Max((x1_i - x3_i)^2)} \tag{3}$$

After comparing all pairs of methods with each other, we get 21 options for the values of *ed* and *edm* for each coordinate. Such a large array of comparative characteristics can be represented as statistical parameters of Table 6.

Table 6. Minimum (Min), average (Avr) and maximum (Max) values of regular divergences (*ed*) and maximal divergences (*edm*) between methods for each coordinate separately

Statistical parameter	*ed*			*edm*		
	***X*, mm**	***Y*, mm**	***Z*, mm**	***X*, mm**	***Y*, mm**	***Z*, mm**
Min	0.24	0.33	0.27	6.90	9.40	7.62
Avr	7.31	19.45	16.46	137.62	400.88	365.81
Max	14.72	38.02	36.91	388.30	995.11	1027.53

The X coordinate has the smallest statistical differences between the methods in Table 6. In general, the Z-coordinate has slightly less variation than the Y-coordinate. More clearly, the regular divergences between the methods for individual coordinates can be shown graphically (Figure 4).

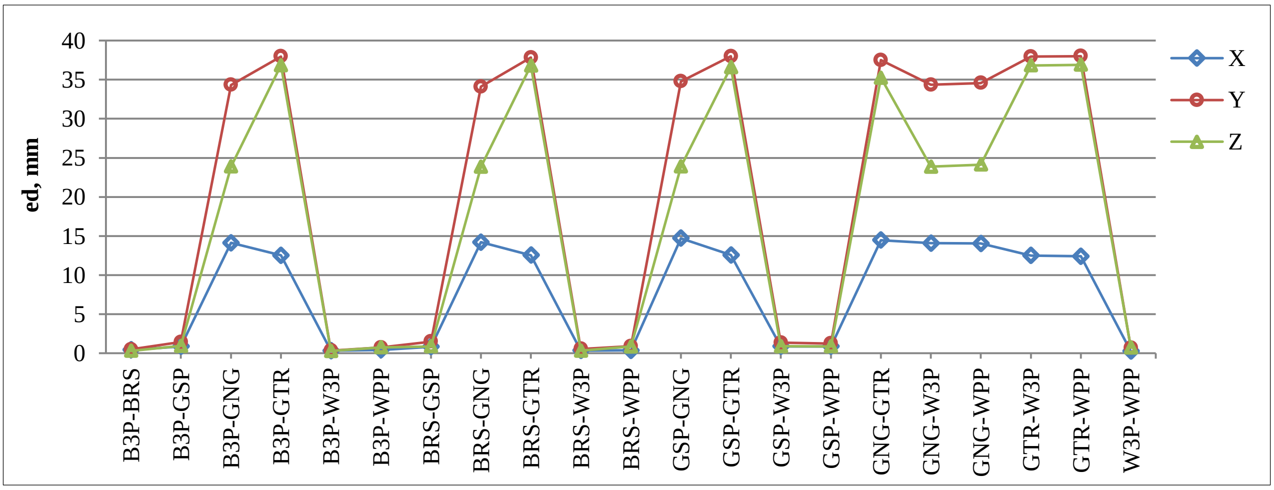

Figure 4. Regular divergences in individual coordinate X-Y-Z for all paired combinations of calculation methods

The level of *ed* values for X is ~2 times less than for other coordinates. The *ed* values for Y and Z are roughly equal, but Z has a slight advantage. Figure 4 indicates the same group of methods (B3P, BRS, GSP, W3P, WPP) with *ed*<1.5 mm. The maximal divergences by individual coordinates between the methods have the following graphical illustration (Figure 5).

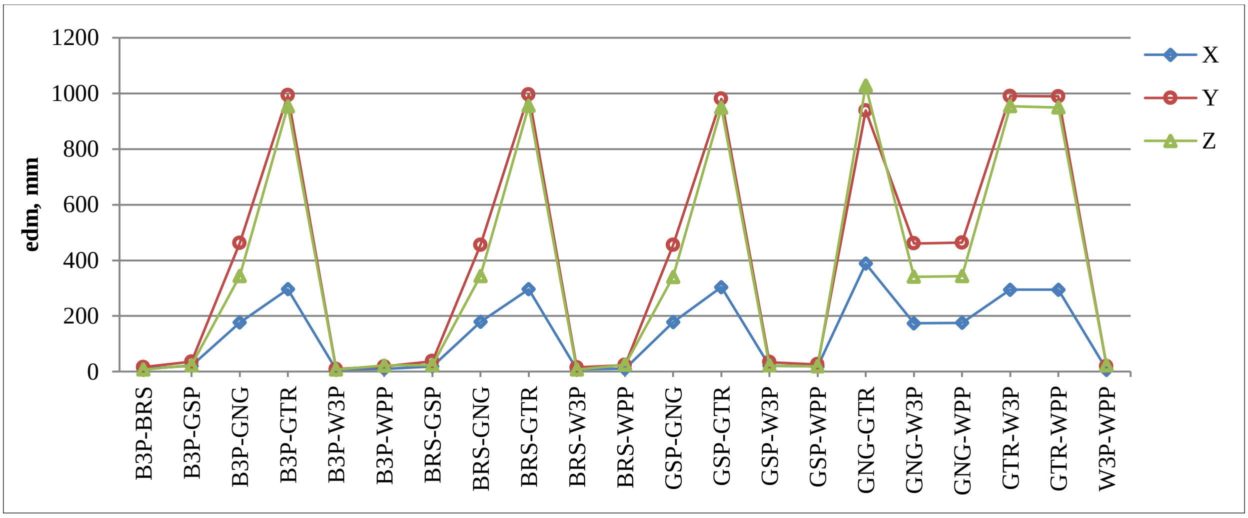

Figure 5. Maximal divergences for individual X-Y-Z coordinates for all paired combinations of calculation methods

Figures 4 and 5 are similar in form, but the *ed* value is up to 40 mm, and the *edm* reaches 1 meter. In Figure 5, the wave tops are sharper because the GNG method has a slightly better coordinate calculation than on Figure 4. Also the 5 methods have relatively low *edm* <38 mm in Figure 5.

4.3. Differences in the Positioning Methods on XYZ Coordinates of Individual Stations

Each station has different positioning errors when processing GNSS observation data. This may be due to the geometry of the constellation of satellites above the station, limited visibility of the satellites, signal refraction, etc. Let us make an indirect assessment of the quality of the signal received by the GNSS station based on the divergence of coordinates calculated by 7 methods. The smaller the divergence of coordinates for one station in different calculation methods, the better the GNSS information is recorded by the receiver. In this case, for each station a series of 24 values is formed (3 coordinates × 8 days), as shown in Table 7.

Table 7. Coordinate pairs calculated by different methods for each station

Method code, coordinate	XYZ coordinate series for *S1* station								
B3P, *C1*	$x1^{S1}_{D1}$	$x1^{S1}_{D2}$	…	$y1^{S1}_{D1}$	$y1^{S1}_{D2}$	…	$z1^{S1}_{D1}$	…	$z1^{S1}_{D8}$	*ED*, *ed*, *edm*
GSP, *C3*	$x3^{S1}_{D1}$	$x3^{S1}_{D2}$	…	$y3^{S1}_{D1}$	$y3^{S1}_{D2}$	…	$z3^{S1}_{D1}$	…	$z3^{S1}_{D8}$	

Thus, 21 variants of similar tables with the corresponding parameters *ed* and *edm* for each station will be formed. The POL2 station has the lowest XYZ coordinates divergence with the following values (Table 8).

Table 8. Regular (*ed*) and maximal (*edm*) divergences in XYZ coordinates between method pairs for POL2 station

***ed*, mm** / ***edm*, mm**	**B3P**	**BRS**	**GSP**	**GNG**	**GTR**	**W3P**	**WPP**
B3P		0.66	1.48	47.00	2.93	0.44	0.65
BRS	11.07		1.52	46.70	3.10	0.64	1.00
GSP	15.09	17.83		47.19	3.23	1.59	1.68
GNG	457.06	445.99	454.55		45.88	46.89	47.41
GTR	25.56	28.12	32.29	450.17		3.04	3.13
W3P	4.39	11.38	15.79	457.37	25.30		0.67
WPP	8.07	13.28	14.06	459.27	25.70	8.00	

The *ed* and *edm* values related to the GNG method are an order of magnitude greater than other values of Table 8. But the GTR method had the worst such parameters in the previous sections. In case of POL2, the GTR method has the lowest *ed* and *edm* because this station acted as the PRF for the GTR method.

The POL3 has the highest level of coordinate divergence between methods, although this station is located 900 m from POL2 (Table 9).

Table 9. Parameters of coordinate divergences between method pairs for POLY 3 station

ed, mm / *edm*, mm	B3P	BRS	GSP	GNG	GTR	W3P	WPP
B3P		0.66	1.48	47.00	2.93	0.44	0.65
BRS	11.07		1.52	46.70	3.10	0.64	1.00
GSP	15.09	17.83		47.19	3.23	1.59	1.68
GNG	457.06	445.99	454.55		45.88	46.89	47.41
GTR	25.56	28.12	32.29	450.17		3.04	3.13
W3P	4.39	11.38	15.79	457.37	25.30		0.67
WPP	8.07	13.28	14.06	459.27	25.70	8.00	

The biggest difference between Tables 8 and 9 is in the GTR values, the other corresponding values of these tables are comparable. To reduce the amount of tabular information for each station, we present it as average values of *ed* and *edm:*

$$\overline{ed} = \frac{1}{21}\sum_{i=1}^{21} ed_i, \overline{edm} = \frac{1}{21}\sum_{i=1}^{21} edm_i \tag{4}$$

The values calculated by Equation 4 are presented in Table 10.

Table 10. Averaged regular and maximal divergences in XYZ for each station

	IATA	CHUM	KAZA	KRTV	POL2	POL3	POL7	POLY	SUMK	TALA
$\overline{ed}$, mm	17.21	15.17	16.54	15.22	14.61	53.81	15.43	36.72	16.36	17.24
$\overline{edm}$, mm	158.37	146.65	153.43	151.70	141.92	399.32	146.85	280.11	156.18	161.10

The POL2 has the smallest average parameters $\overline{ed} < 15$ mm and $\overline{edm} < 142$ mm in Table 10. The other 7 stations (IATA, CHUM, KAZA, KRTV, POL7, SUMK and TALA) have slightly worse comparison criteria. The POLY and POL3 have several times worse comparison criteria, which may indicate a lower quality of the GNSS signal received by them. Only the GTR and GNG methods contribute to the maximum variation in the positioning of these two stations. The other 5 methods calculate the coordinates for these stations quite precisely.

5. Divergence for UVW Coordinates in Local Reference Frame

The geocentric XYZ coordinates are determined with a different number of external corrections for the current day using different calculation methods. Different methods and reference frames have different effects on station positioning errors. The farther the studied stations are located from the observer or Reference Frame, the greater the positioning errors become. In such cases, the increments in XYZ coordinates for stations from one day to the next may be greater than the increments in line lengths between these stations in these days. To reduce positioning errors, the transformation of global XYZ coordinates into a Local Reference Frame (LRF) is used. Such procedure for transformation of reference frame for coordinates of a station group is described in Ischuk et al. [22]. The actual reduction in the level of coordinate variations reached 17% as a result of such coordinate transformation in Kenigsberg et al. [19].

5.1. Divergences of Radius Vectors from Different Methods in LRF

To transform global XYZ coordinates into local UVW, it is necessary to change the reference frame (Figure 2). For each method of calculating the coordinates, it is necessary to place the observer in the average position of 10 studied stations per day (point L, Figure 2). For example, the X coordinate for point L of one day and one method will be calculated:

$$x_L = \frac{1}{10}(x_{IATA} + x_{CHUM} + \cdots + x_{TALA}) \tag{5}$$

The average positions for point L for y and z are calculated in the same way. Then the coordinates of the stations in the LRF for each day and each method will be calculated:

$$u = x - x_L, v = y - y_L, w = z - z_L \tag{6}$$

Next, we will form 80 pairs of radius vectors $\vec{V}(u, v, w)$ for each pair of positioning methods according to the Table 2 principle. The values of Euclidean distances, regular and maximal divergences between the methods by 3D vectors were calculated using Equations 1 and 2 adapted to UVW coordinates and entered in Table 11.

Table 11. The regular and maximal divergences for pair of positioning methods by radius vectors in LRF

***ed*, mm** / ***edm*, mm**	**B3P**	**BRS**	**GSP**	**GNG**	**GTR**	**W3P**	**WPP**
B3P		0.64	1.09	1.30	45.84	0.46	0.99
BRS	20.95		1.06	1.18	45.73	0.60	1.07
GSP	22.99	23.55		0.67	45.64	1.01	0.79
GNG	38.51	29.90	25.63		45.57	1.25	1.04
GTR	1118.30	1117.75	1112.79	1110.13		45.79	45.67
W3P	9.07	20.84	23.31	38.87	1113.67		0.91
WPP	23.38	22.81	26.12	42.24	1110.69	23.25	

The average levels of regular and maximum divergences for the radius vectors in XYZ coordinates were 26.6 and 283.2 mm, respectively (Table 3). The same characteristics are $\overline{ed} = 13.7$ mm and $\overline{edm} = 175.3$ mm in Table 11. So, the average divergences of radius vectors decreased by 1.6-2 times after the transformation of global XYZ into local UVW coordinates.

The GNG method in UVW coordinates has relatively low divergence values and is included in the group of methods with *ed*<1.3 mm and *edm*<43 mm (Table 10). Therefore, XYZ coordinates with RRF have less accuracy of reference on a global scale, but their transformation into LRF significantly increases the precision of relative positioning between stations. Thus, XYZ coordinates with RRF have less reference accuracy on a global scale, but their transformation into LRF significantly increases the precision of relative positioning between stations. Only the GTR method with PRF reduced the divergence slightly when transforming coordinates to LRF, from Table 3 to Table 11.

5.2. Coordinate Divergence along Individual U-V-W Axes

By analogy with the data ordering process for comparing coordinates by individual X-Y-Z axes (Table 5), tables were made and *ed* and *edm* parameters were calculated for each U-V-W axis separately. Each coordinate corresponds to 21 pairs of *ed* and *edm* values, the statistical characteristics of which are presented in Table 12.

Table 12. Statistical characteristics for *ed* and *edm* on separate coordinates U-V-W in LRF

Statistical parameter	***ed***			***edm***		
	***U*, мм**	***V*, мм**	***W*, мм**	***U*, мм**	***V*, мм**	***W*, мм**
Min	0.19	0.28	0.23	6.25	6.99	6.43
Avr	2.93	9.66	9.28	79.72	237.60	230.42
Max	9.43	32.48	30.94	248.42	794.80	757.80

The coordinate axes are arranged in the order X-Z-Y and U-W-V according to the value spread from method to method in Tables 6 and 12. But local UVW coordinates have 1.5 times less divergences between methods than global XYZ. Graphs of *ed* and *edm* for individual U-W-V coordinates from different methods differ from analogues in figures 4 and 5 only by the GNG method.

5.3. Differences in the Positioning Methods on UVW Coordinates of Individual Stations

In accordance with section 4.3 (XYZ), we performed the same actions for the UVW coordinates of individual stations. Average values of regular and maximum divergences between methods for each station are shown in Table 13.

Table 13. Averaged regular and maximal divergences in UVW for each station

Parameter	**IATA**	**CHUM**	**KAZA**	**KRTV**	**POL2**	**POL3**	**POL7**	**POLY**	**SUMK**	**TALA**
$\overline{ed}$, mm	4.99	8.03	6.04	8.77	8.82	35.44	7.42	18.21	7.01	5.68
$\overline{edm}$, mm	34.82	54.47	43.36	74.84	62.16	230.14	49.08	132.52	50.66	44.79

When transforming global into local coordinates, the values of Table 13 (UVW) were reduced by >2 times compared to Table 10 (XYZ). The greatest contribution to the reduction of divergence was made by the GNG method. The stations are arranged in the same order in terms of the quality of the received GNSS signal ($\overline{ed}$ and $\overline{edm}$) in XYZ (Table 10) and in UVW (Table 13).

6. Discussions and Conclusions

The average level of modern displacements of the earth's crust in Central Asia, according to GNSS measurements, does not exceed a few millimeters per year [3–6]. At the same time, the determination of the geodetic positions of GNSS stations is also determined at approximately the same level of accuracy [8]. Therefore, the accuracy of calculating the average daily coordinates of stations is important in construction work and the monitoring of important man-made objects in long-term geodynamic studies. One of the important issues for us is the choice of a tool, method, and algorithm for the most accurate detection of crustal movements in the Central Asian region, in particular in Kyrgyzstan. In this paper, the emphasis is on the processing and analysis of GNSS measurement data.

It is known from our experience and other works that, under equal initial conditions, the best accuracy of spatial GNSS positioning is provided by the GAMIT/GLOBK and Bernese software packages. The differences in the coordinates and velocity vectors calculated by them usually do not exceed a few millimeters, but in some cases they reach a few centimeters [9, 15, 17, 18]. All these comparisons are made without the presence of reference values, so there is no good reason to give preference to any program. Note that an increased RMS value for station coordinates is only an indirect sign of poor positioning quality. During measurements, there may be real GNSS antenna offsets, which will increase the coordinate RMS.

At the moment, the issue of choosing a GNSS constellation to ensure the maximum accuracy of daily positioning is almost unambiguously resolved in favor of GPS without the complex use of other constellations [9, 10, 12, 15]. For analysis, we chose GPS measurements under favorable conditions at 10 stations in Central Asia for 8 days in different seasons. We performed all pairwise comparisons for 7 sets of XYZ coordinates calculated by different methods based on the same input GPS data. These 7 sets of XYZ coordinates are obtained by 3 different methods inside GAMIT/GLOBK, 2 algorithms inside the Bernese program, and 2 web services (CSRS-PPP and APPS). We are not aware of studies on the analysis of different methods for calculating coordinates within the GAMIT/GLOBK and Bernese programs, taking into account their various settings and connections with different reference frames.

All 7 studied sets of daily XYZ coordinates differ from each other, which confirms the difference in the algorithms for their calculation. To compare 2 sets of 3D coordinates, corresponding evaluation parameters are required. If RMS is used as a criterion, then first it must be calculated for a number of differences $\Delta X_i = X1_i - X2_i$, then for all $\Delta Y_i = Y1_i - Y2_i$and for all $\Delta Z_i = Z1_i - Z2_i$. Pair combinations for 7 sets multiplied by 3 coordinates form 63 RMS, each of which will characterize only one coordinate for one pair of sets. In addition, in this case, the maximum differences in coordinates are not taken into account.

To reduce the volume of comparative parameters and generalize the approach for comparing coordinate sets, it is proposed to use the Euclidean distance between them. If we divide the distance between 2 sets in a multidimensional space by the dimension of this space, then we obtain an estimate of the average distance per one dimension of the space *ed* (3). In fact, this is a special average estimate of the difference between 2 corresponding coordinates of 2 compared samples. The maximum value of the root of the squared difference of the 2 compared coordinates will give an estimate of the maximum difference of the 2 samples *edm* (3). Recall that the compared coordinate samples characterize the same position in a multidimensional space by different methods. Therefore, it can be assumed that the true value of this position is between these multidimensional vectors (samples) or within the Euclidean distance between them. When comparing coordinate samples, the parameter *ed* will characterize the target accuracy, and the maximum value *edm* will evaluate precision.

In the logic of this approach, the coordinates as elementary members of the compared samples (3) can be replaced by radius vectors (2). We can form samples for comparison from all coordinate types, but in a given order and in logical correspondence with each other. At the same time, it is important to take into account the expediency of such a combination and the comparability of the measurement units for all formed sample members. The parameters of regular (*ed*) and maximum (*edm*) divergence of coordinates can be used to estimate differences between samples, and their quantitative indicators are comparable with other estimation parameters.

In analysis result, we evaluated the coordinate reproducibility by different methods in the global (ITRF), regional (RRF), point (PRF), and local (LRF) reference frames. For the most accurate reference of stations in geocentric XYZ coordinates, it is best to use the standard calculation methods from the Bernese (B3P, BRS) and GAMIT/GLOBK (GSP) programs, as well as the W3P and WPP online services. These methods use ITRF and have regular radius vector differences <2 mm, single maximum discrepancies up to 45 mm. Our results are well comparable with individual works in this direction [15, 18]. The GNG and GTR (GAMIT/GLOBK) methods use the regional (RRF) and point (PRF) reference frames, which negatively affects the quality of snapping in XYZ coordinates compared to the methods for computing coordinates in ITRF.

Based on the overall averages *ed* and *edm* from tables 3 (XYZ) and 11 (UVW), the studied methods are ranked from minimum to maximum values in the following order: W3P, B3P, BRS, WPP, GSP, GNG, GTR. The first 4 places with the minimum values of accuracy and precision are occupied by methods based on the "Precise Point Positioning" (PPP) algorithm. Using the general principles of this algorithm, they provide sufficiently close to each other coordinate sets. In terms of weighted quantities of same type solutions, they pushed high-quality standard processing method of

GAMIT/GLOBK (GSP) to 5th place with a minimal difference in the evaluation parameters. Here the web service "Canadian Spatial Reference System Precise Point Positioning" has a slightly better accuracy score than Bernese's PPP method. Since we do not have coordinate references to more confidently compare calculation methods, Bernese's PPP method and GAMIT/GLOBK's standard processing method still have a high accuracy rating. These software methods are still indispensable for mass autonomous calculations of average daily coordinates with the ability to customize the algorithms. However, it should be noted that the two studied web services (CSRS-PPP and APPS) are able to compete with well-known software in the field of solving average daily coordinates.

Converting XYZ coordinates to UVW with LRF reduces the average level of discrepancies between UVW coordinates of all methods by >1.5 times. Such a transformation improves the precision of the UVW coordinates, but may degrade their accuracy with respect to ITRF. The GNG method initially had RRF, therefore, with the methods in ITRF, it had discrepancies in radius vectors of ⩾45 mm. But in UVW coordinates, the GNG method began to be included in the group of methods with minimal differences in the coordinate divergence parameters. Only the GTR method in UVW coordinates has significant discrepancies (*ed*<46 mm and *edm*<1.2 m) compared to other methods. But this calculating intraday coordinates method is for stations distant <100 km, and in our case the stations are farther away.

As the values of *ed* and *edm* increase, the coordinate axes are arranged in the following order: X-Z-Y and U-W-V. The X and U coordinates have a 2-3 times lower level of discrepancies from method to method due to the orientation of the coordinate axes with respect to the location of the stations under study. The closer the coordinate axis is to the direction of the station under study, the worse the accuracy of calculating the values along this coordinate axis for this station will be.

A comparison of positioning methods for each individual station can provide a quality assessment of the received GNSS information. If the station has a lower level of coordinate divergences from method to method, the data it records is of higher quality. In our case, the eight studied stations have a reproducibility of XYZ and UVW coordinates that is 2-3 times better than the other two.

7. Declarations

7.1. Author Contributions

Conceptualization, S.K.; methodology, S.K.; software, D.K., Y.S., and O.P.; validation, D.K., Y.S., and O.P.; formal analysis, S.K. and D.K.; investigation, S.K. and D.K.; resources, D.K., Y.S., and O.P.; data curation, D.K., Y.S., and O.P.; writing—original draft preparation, S.K. and D.K.; writing—review and editing, S.K. and D.K.; visualization, S.K. and D.K.; supervision, S.K.; project administration, S.K.; funding acquisition, S.K. All authors have read and agreed to the published version of the manuscript.

7.2. Data Availability Statement

The initial data for calculating coordinates in this study for 10 stations over 8 days of measurements (80 RINEX files) are publicly available in the FigShare repository [https://doi.org/10.6084/m9.figshare.21118912.v1].

7.3. Funding

The research was carried out within the framework of topics for the Research station of RAS in Bishkek city (AAAA-A19-119020190066-3, AAAA-A20-120102190010-5).

7.4. Acknowledgements

The authors thank the staff of the Research station of RAS who took part in the process of GPS measurements at the stations indicated in the study.

7.5. Conflicts of Interest

The authors declare no conflict of interest.

8. References

[1] Mousavi, S. M., Shamsai, A., El Naggar, M. H., & Khamehchian, M. (2001). A GPS-based monitoring program of land subsidence due to groundwater withdrawal in Iran. Canadian Journal of Civil Engineering, 28(3), 452–464. doi:10.1139/cjce-28-3-452.

[2] Mayunga, S. D., & Bakaone, M. (2021). Dynamic Deformation Monitoring of Lotsane Bridge Using Global Positioning Systems (GPS) and Linear Variable Differential Transducers (LVDT). Journal of Data Analysis and Information Processing, 09(01), 30–50. doi:10.4236/jdaip.2021.91003.

[3] Zubovich, A. V., Wang, X. Q., Scherba, Y. G., Schelochkov, G. G., Reilinger, R., Reigber, C., Mosienko, O. I., Molnar, P., Michajljow, W., Makarov, V. I., Li, J., Kuzikov, S. I., Herring, T. A., Hamburger, M. W., Hager, B. H., Dang, Y. M., Bragin, V. D., & Beisenbaev, R. T. (2010). GPS velocity field for the Tien Shan and surrounding regions. Tectonics, 29(6), 6014. doi:10.1029/2010TC002772.

[4] Zhou, Y., He, J., Oimahmadov, I., Gadoev, M., Pan, Z., Wang, W., Abdulov, S., & Rajabov, N. (2016). Present-day crustal motion around the Pamir Plateau from GPS measurements. Gondwana Research, 35, 144–154. doi:10.1016/j.gr.2016.03.011.

[5] Kuzikov, S. I., & Mukhamediev, S. A. (2010). Structure of the present-day velocity field of the crust in the area of the Central-Asian GPS network. Izvestiya, Physics of the Solid Earth, 46(7), 584–601. doi:10.1134/S1069351310070037.

[6] Qiao, X., Yu, P., Nie, Z., Li, J., Wang, X., Kuzikov, S. I., Wang, Q., & Yang, S. (2017). The Crustal Deformation Revealed by GPS and InSAR in the Northwest Corner of the Tarim Basin, Northwestern China. Pure and Applied Geophysics, 174(3), 1405–1423. doi:10.1007/s00024-017-1473-6.

[7] Inal, C., Bulbul, S., & Bilgen, B. (2018). Statistical analysis of accuracy and precision of GNSS receivers used in network RTK. Arabian Journal of Geosciences, 11(10), 227 1–8. doi:10.1007/s12517-018-3581-8.

[8] Kuzikov, S. I. (2014). Methodical questions and accuracy problems of GPS observations by the example of the geodynamic proving ground in Bishkek. Izvestiya, Physics of the Solid Earth, 50(6), 770–784. doi:10.1134/S1069351314060032.

[9] Jivall, L., Nilfouroushan, F., & Al Munaizel, N. Analysis of 20 years of GPS data from SWEREF consolidation points – using BERNESE and GAMIT-GLOBK software. Reports in Geodesy and Geographical Information Systems. Typography and layout Rainer Hertel, Gävle, Sweden, 1-84. doi:10.13140/RG.2.2.25918.97609.

[10] Atiz, Ö. F., Konukseven, C., Öğütcü, S., & Alçay, S. (2021). Comparative analysis of the performance of Multi-GNSS RTK: A case study in Turkey. International Journal of Engineering and Geosciences, 7(1), 67–80. doi:10.26833/ijeg.878236.

[11] Yatskiv, Y., Khoda, O., Ishchenko, M., & Zhalilo, O. (2021). The Research Activities of the Main Astronomical Observatory of the National Academy of Sciences of Ukraine on the Use of GNSS Technology. Kinematics and Physics of Celestial Bodies, 37(2), 96–105. doi:10.3103/S0884591321020069.

[12] Galaganov, O. N., Guseva, T. V., & Krupennikova, I. S. (2015). Comparison of GLONASS and GPS data by differential positioning method in static mode for solving geodynamic problems. Sovremennye Problemy Distantsionnogo Zondirovaniya Zemli Iz Kosmosa, 12(4), 28–37.

[13] Herring, T. A., King, R. W., Floyd, M. A., & McClusky, S. C. (2010). Introduction to GAMIT/GLOBK: Release 10.7". Massachusetts Institute of Technology.

[14] Dach, R., Hugentobler, U., Fridez, P., & Meindl, M. (2007). Bernese GPS Software Version 5.0, Astronomical Institute. University of Bern, Bern, Switzerland. doi:10.7892/boris.72297.

[15] Shestakov, N. V., Sysoev, D. V., Gerasimenko, M. D., Titkov, N. N., Verkhoturov, A. L., Gagarskii, N. A., Kishkina, A. K., Guojie, M., & Takahashi, H. (2019). On determination of the Earth's surface small "instant" vertical displacements by GNSS-techniques. Sovremennye Problemy Distantsionnogo Zondirovaniya Zemli Iz Kosmosa, 16(4), 33–44. doi:10.21046/2070-7401-2019-16-4-33-44.

[16] Montenbruck, O., Steigenberger, P., & Hauschild, A. (2018). Multi-GNSS signal-in-space range error assessment – Methodology and results. Advances in Space Research, 61(12), 3020–3038. doi:10.1016/j.asr.2018.03.041.

[17] Gandolfi, S., Macini, P., Poluzzi, L., & Tavasci, L. (2020). GNSS measurements for ground deformations detection around offshore natural gas fields in the Northern Adriatic Region. Proceedings of the International Association of Hydrological Sciences, 382, 89–93. doi:10.5194/piahs-382-89-2020.

[18] Premužić, M., Đapo, A., Bačić, Ž., & Pribičević, B. (2020). Accuracy Analysis of Point Velocities Determined by Different Software Packages and GNSS Measurement Processing Methods. Tehnički Glasnik, 14(4), 446–457. doi:10.31803/tg-20200515225239.

[19] Kenigsberg, D. V., Salamatina, Y. M., Prokhorov, O. A., & Kuzikov, S. I. (2021). Convergence of daily mean coordinates of precise positioning methods. IOP Conference Series: Earth and Environmental Science, 929(1), 12014. doi:10.1088/1755-1315/929/1/012014.

[20] CSRS-PPP (2023). Canadian Spatial Reference System Precise Point Positioning, CSRS-PPP, Canada. Available online: https://webapp.geod.nrcan.gc.ca/geod/tools-outils/ppp.php?locale=en (accessed on January 2023).

[21] GDGPS (2022). Jet Propulsion Laboratory. The Automatic Precise Point Service of the Global Differential GPS System, APPS. California Institute of Technology, Pasadena, United States. Available online: https://apps.gdgps.net (accessed on January 2023).

[22] Ischuk, A., Bendick, R., Rybin, A., Molnar, P., Khan, S., Kuzikov, S., Mohadjer, S., Saydullaev, U., Ilyasova, Z., Gennady Schelochkov, G., & Zubovich, A.V. (2013). Kinematics of the Pamir and Hindu Kush regions from GPS geodesy. Journal of Geophysical Research: Solid Earth, 118, 2408–2416. doi:10.1002/jgrb.50185.

[23] Sokal, R. R., & Michener, C. D. A. (2009). Statistical method for evaluating systematic relationships. University of Kansas Scientific Bulletin, 38(22), 1409–1438.

[24] Odell, P. L., & Duran, B. S. (1974). Cluster Analysis. Lecture Notes in Economics and Mathematical Systems, Springer-Verlag, Berlin, Germany. doi:10.1007/978-3-642-46309-9.